



How sensitive is tropospheric oxidation to anthropogenic emissions?

Oliver Wild¹ and Paul I. Palmer²

Received 15 August 2008; revised 3 October 2008; accepted 8 October 2008; published 18 November 2008.

[1] We use a global chemistry transport model to explore how changes in anthropogenic emissions alter ozone production and tropospheric oxidizing capacity over decadal (1990–2010) and centennial timescales (1900–2100). We find that the spatial extent of O₃ production and loss in the troposphere changes very little despite large projected increases in precursor emissions. While tropospheric OH shows a long-term decrease of only 20% between 1900 and 2100, there are widespread changes in distribution which alter regional oxidation capacity substantially. We show that the remote marine boundary layer remains an important net sink of O₃, as greater production related to increased continental NO_x emissions is outweighed by greater O₃ destruction. The critical NO_x level required to support net O₃ production doubles between 1900 and 2100, from 28 to 55 pptv on average, preventing any large-scale shift in production regime. **Citation:** Wild, O., and P. I. Palmer (2008), How sensitive is tropospheric oxidation to anthropogenic emissions?, *Geophys. Res. Lett.*, 35, L22802, doi:10.1029/2008GL035718.

1. Introduction

[2] The lifetime of many pollutants in the global troposphere is governed by the abundance of the hydroxyl radical (OH). Photolysis of ozone (O₃) is the primary source of OH in the troposphere, and consequently the concentration and distribution of O₃ has important implications for the removal of these pollutants. Tropospheric O₃ is produced by the oxidation of CO, CH₄ and volatile organic compounds (VOCs) in the presence of nitrogen oxides (NO_x = NO + NO₂) and is lost by both chemical and physical processes with a lifetime of weeks to months [e.g., Prather *et al.*, 2001]. The balance between O₃ production (P) and loss (L) is determined by the relative abundance of NO_x and VOCs and varies with geographical location and season. The continental boundary layer is typically a net source of O₃ except in regions of intense NO emissions in wintertime. The marine boundary layer is generally a net O₃ sink, reflecting high humidity and a low abundance of NO_x [Reeves *et al.*, 2002; DiNunno *et al.*, 2003], although net production may occur in coastal regions influenced by continental pollutant outflow.

[3] Increasing anthropogenic emissions of NO_x, CO and VOCs have led to large increases in tropospheric O₃ over the past century [e.g., Wang and Jacob, 1998], and this trend is likely to continue [Prather *et al.*, 2003; Stevenson *et al.*, 2006]. This greater O₃ abundance alters the photochem-

ical environment of the global troposphere by changing the supply of oxidants, and may alter patterns of O₃ production and loss. Previous model studies have focussed on changing radiative forcing or continental air quality but relatively few have explored changes in the oxidizing capacity of the troposphere [e.g., Brasseur *et al.*, 1998; Lelieveld *et al.*, 2002]. We focus here on changing oxidation and in particular on how photochemistry over clean oceanic regions, which we find to be responsible for almost 50% of chemical O₃ destruction in the global troposphere, may evolve as O₃ precursor emissions increase. Increases in marine background O₃ concentrations have been observed over eastern parts of the Pacific (0.3–0.8 ppbv yr⁻¹) [Jaffe *et al.*, 2003; Parrish *et al.*, 2004] and Atlantic (0.05–0.7 ppbv yr⁻¹) [Lelieveld *et al.*, 2004; Derwent *et al.*, 2007] oceans, and have been attributed to increased anthropogenic emissions of O₃ precursors. Recent analysis of ground-based and aircraft campaign data over the eastern mid-latitude Pacific between 1984 and 2002 suggests that the North Pacific is becoming less of an O₃ sink [Parrish *et al.*, 2004]. If the marine troposphere becomes less efficient in removing tropospheric oxidants, the effects of increasing anthropogenic emissions will be amplified, with potentially disastrous consequences for continental air quality.

2. Modelling O₃ Production

[4] We use the Frontier Research System for Global Change version of the University of California, Irvine (FRSGC/UCI) global 3-D chemistry-transport model (CTM) [Wild and Prather, 2000; Wild *et al.*, 2004] to examine the evolution of tropospheric photochemistry over decadal (1990–2000–2010) and centennial (1900–2000–2100) time scales. The CTM is run at T21 resolution (5.6° × 5.6°) with ECMWF meteorology for 1996. The five simulations described here use the same 1996 meteorology so that year-to-year variations in atmospheric transport do not influence the results. We discuss later how changes in meteorology and climate may affect our results.

[5] Emission data for 2000, 2010 and 2100 are based on the SRES A2p scenario [Prather *et al.*, 2001], and for 1900 are based on the EDGAR-HYDE dataset v1.3 [van Aardenne *et al.*, 2001] (Table 1). Emissions for 1990 are derived by applying a regional scaling to 2000 emissions based on changes in liquid fuel CO₂ usage for CO and VOCs and changes in total CO₂ usage for NO_x [Marland *et al.*, 2006]. Natural sources are held constant for 1990–2100, but soil and biomass burning sources, which are heavily influenced by human activities, are reduced for 1900 following EDGAR-HYDE. A uniform distribution of CH₄ was used in each scenario, with the abundance fixed at 900 ppbv in 1900 and 3730 ppbv in 2100 [Prather *et al.*, 2001]. Simulated present-day O₃ production and loss rates have been evaluated against observation-based rates derived with a photochemical

¹Department of Environmental Science, Lancaster Environment Centre, Lancaster University, Lancaster, UK.

²School of GeoSciences, University of Edinburgh, Edinburgh, UK.

Table 1. Trace Gas Emissions

	1900	1990	2000	2010	2100
<i>NO_x (Tg N/yr)</i>					
Fossil fuel	2.0	31.6	31.8	38.9	109.0
Biomass burning	2.9	6.2	6.2	6.2	6.2
Lightning	5.0	5.0	5.0	5.0	5.0
Soil	2.9	5.6	5.6	5.6	5.6
Aircraft ^a	0.0	0.5	0.7	1.0	2.2
Stratosphere (NO _y)	0.5	0.5	0.5	0.5	0.5
Total	13.3	49.4	49.8	57.2	128.5
<i>CO (Tg CO/yr)</i>					
Fossil fuel	96	649	650	750	2098
Biomass burning	229	496	496	496	496
Vegetation/ocean	200	200	200	200	200
Total	525	1345	1346	1445	2794
<i>VOC (Tg species/yr)</i>					
Fossil fuel	17	201	201	214	402
Biomass burning	15	42	42	42	42
Isoprene	453	453	453	453	453
Total	485	696	696	709	897
<i>CH₄ (ppbv)</i>					
Uniform distribution	900	1700	1760	1860	3730

^a2050 projections used for 2100 scenario.

steady-state box model constrained by aircraft measurements (see auxiliary material¹). The CTM reproduces these observation-based rates to within about 0.5 ppbv/day over marine regions, but underestimates boundary layer production close to East Asia, likely reflecting underestimation of O₃ precursor emissions [Palmer *et al.*, 2003] and limitations associated with model resolution. A more detailed analysis of the biases in simulating O₃ production is given by Wild *et al.* [2004].

3. Evolution of Tropospheric Oxidation

[6] Table 2 summarises changes in the photochemical environment of the troposphere between 1900 and 2100. The rates of O₃ production and loss increase by about a factor of three between 1900 and 2100, and the tropospheric O₃ burden doubles. Mean surface O₃ over the continents increases by 30 ppbv between 1900 and 2100; the 16 ppbv increase from 2000 to 2100 is comparable to that seen in previous multi-model studies using SRES A2 emission projections [Prather *et al.*, 2003]. Surface deposition is greatly increased, while influx from the stratosphere is marginally reduced due to a weaker cross-tropopause O₃ gradient. The net effect of these changes is that the troposphere shifts from being a net sink of O₃ of 40 Tg yr⁻¹ to being a net source of 740 Tg yr⁻¹. The chemical lifetime of O₃ in the boundary layer is reduced by 25% from 12 days in 1900 to 9 days in 2100, and the mean global tropospheric lifetime drops by a similar amount, from 25 to 19 days.

[7] Figure 1 shows the global distribution of annual mean net O₃ production. Although NO_x emissions increase by an order of magnitude between 1900 and 2100, the regions of net production and loss remain remarkably constant, even though the magnitudes of production and destruction within each regime increase greatly. The tran-

sitions to net production in regions of continental or convective outflow are very limited in extent and are largely offset by reduced net production at high latitudes where the effect of shorter O₃ lifetime dominates. Net O₃ destruction occurs over 56% of the troposphere by mass, and this remains constant between 1900 and 2100 suggesting that changes in production and loss are well balanced and that the chemical regimes in the troposphere remain strongly buffered.

[8] The constancy of the distribution of O₃ production and loss regimes reflects the interaction of changes in chemical lifetime with atmospheric transport. The greater abundance of O₃ and its precursors in 2100 supports more active photochemistry in many parts of the troposphere, and in turn its shorter lifetime reflects an increased abundance of HO₂. While emissions of NO_x increase ten-fold from 1900, the tropospheric burden increases by only a factor of three as NO_x removal is greater; the mean tropospheric lifetime drops from 50 to 15 hours, limiting the extent of its redistribution from source regions. This lifetime reduction is driven by the increasing importance of NO_x self-reactions and PAN formation under high-emission conditions. Oxidation of CO, CH₄ and VOCs increases the abundance of peroxy radicals, but the relative increase in O₃ is larger and hence the efficiency of the NO_x catalytic cycle in producing O₃ decreases, from a global average of 0.30 to 0.21 molecules of O₃ per molecule of NO oxidized to NO₂. The number of times a nitrogen atom completes this cycle before oxidation to NO_y is also reduced, from 210 to 95, and consequently the ozone production efficiency (OPE, molecules O₃ produced per molecule NO_x oxidized) is reduced from 65 to 20 on a global basis. These effects are dominated by changes in the continental boundary layer; in the marine boundary layer and free troposphere the reduction in cycling efficiency is smaller (about 10%) and is balanced by increased cycling so that the OPE is relatively constant. Under low-NO_x conditions O₃ production is enhanced, but destruction of the higher background O₃ remains greater so that net production is reduced, see Figure 2. The critical NO_x abundance required to balance the production and loss of O₃ thus increases from 28 to 55 pptv between 1900 and 2100.

[9] How is this stability maintained? Tropospheric oxidation is strongly influenced by the OH radical, and gross production of OH increases by 70% between 1900 and 2000 and by a factor of 3 between 1900 and 2100. These results support and extend those of Lelieveld *et al.* [2002] who

Table 2. Global Tropospheric Trace Gas Budgets (Tg/yr)

	1900	1990	2000	2010	2100
O ₃ Burden (Tg)	226	318	324	337	469
O ₃ Chemistry	-37	292	299	348	736
gross production	2730	4760	4870	5200	8390
gross loss	2770	4470	4570	4850	7650
O ₃ Deposition	479	795	801	847	1210
O ₃ Stratospheric input	516	503	502	500	478
O ₃ Lifetime (days)	25.4	22.1	22.0	21.6	19.3
CH ₄ Chemistry	-311	-521	-543	-581	-1017
CH ₄ Lifetime (yrs)	8.2	9.2	9.1	9.0	10.3
Mean surface O ₃ (ppbv)	16.5	26.7	26.9	28.1	38.8
over continents	20.0	35.2	35.0	36.9	51.2
over open ocean	14.5	21.9	22.3	23.1	31.9

¹Auxiliary materials are available in the HTML. doi:10.1029/2008GL035718.

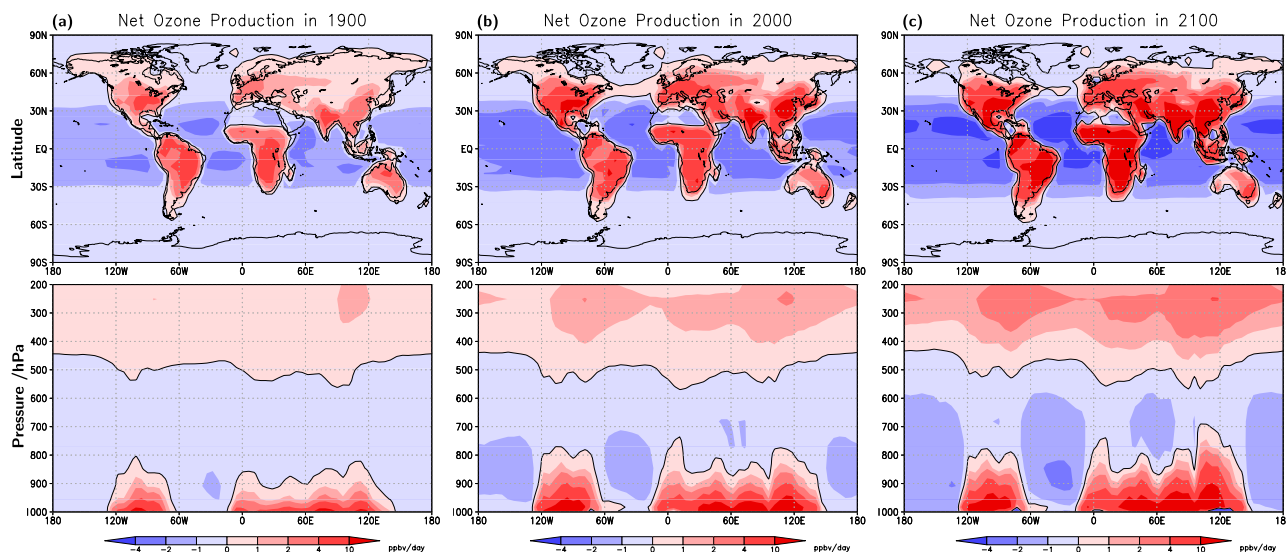


Figure 1. Annual mean distribution of net O_3 production in ppbv/day in (top) the boundary layer and (bottom) at northern mid-latitudes ($20\text{--}60^\circ\text{N}$) in (a) 1900, (b) 2000, and (c) 2100. The contour line marks zero net production.

found a 60% increase since preindustrial times based on 1990 emissions. Primary production is greatest in the humid tropical marine boundary layer, but recycling of OH during oxidation of CO , CH_4 and VOCs provides a secondary source. In 1900, when reactive carbon levels are low, boundary layer OH is highest over the oceans, see Figure 3. However, much higher reactive carbon levels in 2100 lead to a greater increase in the sink of OH over the oceans than the source, and secondary formation over the continents is greatly enhanced. While global OH is reduced by 20% between 1900 and 2100, consistent with previous studies [e.g., Prather *et al.*, 2001; Shindell *et al.*, 2006] and causing an increase in CH_4 lifetime from 8.2 years to 10.3 years, there is a strong shift in OH abundance from oceanic to tropical continental regions. We find that the proportion of CH_4 oxidation occurring in net O_3 production regimes increases from 20 to 26%, indicating a shift in the location of peroxy radical production towards regions with higher NO_x . While long-lived greenhouse gases such as CH_4 are removed more slowly under 2100 conditions, we note that short-lived reactive VOCs and NO_x will be removed more quickly in polluted continental regions where the abundance of OH increases. However, short-lived trace gases of marine origin, such as dimethyl sulphide, will be removed more slowly under 2100 conditions.

[10] The decadal shifts in tropospheric oxidation are more subtle. Although changes in total emissions are small, there are significant shifts in the distribution of emissions equatorwards towards developing countries, and this leads to increased O_3 formation, as seen in previous studies [Gupta *et al.*, 1998]. We find a small decrease in CH_4 lifetime from 9.2 to 9.0 years between 1990 and 2010 associated with an increase in OH of about $0.1\% \text{ yr}^{-1}$; this runs counter to the centennial trend and highlights the sensitivity of tropospheric oxidation to the location of emissions. Wang *et al.* [2004] found a similar trend in OH ($+0.16\% \text{ yr}^{-1}$) between 1988 and 1997 when neglecting changes in stratospheric O_3 column. Observation-derived trends show a decrease over

this period [Prinn *et al.*, 2001] but may be strongly influenced by meteorological variability.

4. Implications for the Marine Troposphere

[11] Are the changes seen here consistent with long-term measurements over oceanic regions? We find that background O_3 increases by an average of $0.15 \text{ ppbv yr}^{-1}$ between 2000 and 2010 over both the eastern Pacific and Atlantic Oceans, much less than the $0.35 \text{ ppbv yr}^{-1}$ suggested by observations over the past decade [Parrish *et al.*, 2004; Derwent *et al.*, 2007]. O_3 destruction increases by 5% over much of the North Pacific, and we find no evidence to support suggestions that the efficiency of O_3 destruction may be decreasing in this region, or that the photochemical environment has changed substantially [Parrish *et al.*, 2004]. Gross O_3 production over the eastern Pacific is enhanced by 3–4% between 2000 and 2010 due to a similar increase in NO_x abundance maintained by a 6–8% increase in PAN. PAN decomposition makes an important contribu-

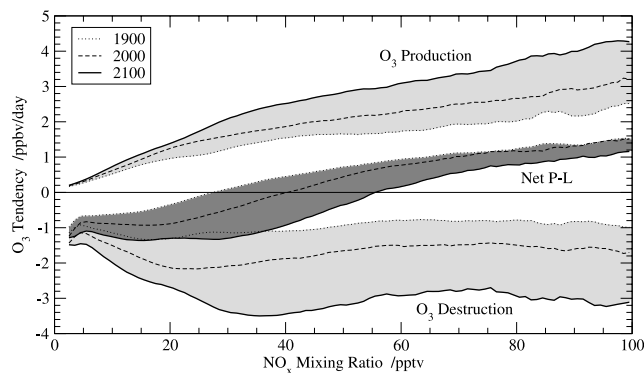


Figure 2. Tropospheric O_3 production and loss rates (ppbv/day) below 250 hPa (10 km) as a function of NO_x (pptv) for 1900, 2000, and 2100. The critical NO_x value for O_3 production occurs where net production (P-L) crosses zero, doubling between 1900 (28 pptv) and 2100 (55 pptv).

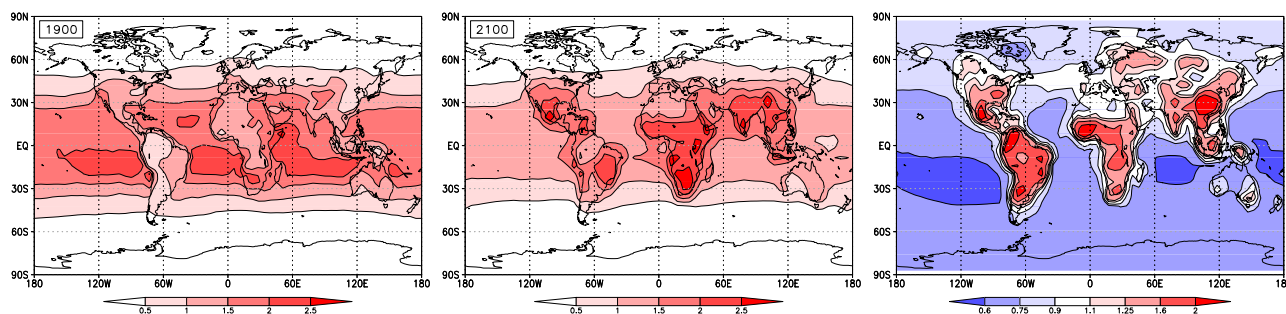


Figure 3. Annual mean distribution of OH (in units of 10^6 molecules cm^{-3}) in the boundary layer in (left) 1900 and (middle) 2100 and the relative change in OH given by (right) the ratio 2100/1900.

tion to O_3 production in this region [Hudman *et al.*, 2004], but we note that increases in PAN remain insufficient to prevent net O_3 destruction increasing even under the polluted 2100 conditions examined here.

[12] Although we find a clear shift towards increased net destruction on a monthly-mean basis, it remains possible that net production occurring during long-range transport of increasingly-polluted continental plumes over the oceans [e.g., Auvray *et al.*, 2007] may continue to increase. Future studies should examine the temporal variability in net production over this region, particularly during transport episodes in springtime. We also note that the present study does not account for recent rapid increases in shipping emissions which enhance O_3 in the marine boundary layer and are likely to reduce net O_3 destruction in coastal regions [Eyring *et al.*, 2007], and may thus contribute to explaining observed trends.

5. Concluding Remarks

[13] We have demonstrated that large projected increases in anthropogenic emissions between 1900 and 2100 have remarkably little effect on the geographical extent of net O_3 production and loss regimes, and thus that the ‘remote’ marine boundary layer remains a large net sink of anthropogenically-induced O_3 . While we find a 20% reduction in global mean OH that indicates that the oxidation capacity of the troposphere is decreasing, redistribution of OH from marine to continental regions leads to substantial changes in regional photochemistry.

[14] In this exploratory study we have considered only a single scenario and have not explored the sensitivity of the results to the balance of NO_x and VOC emissions or CH_4 . We have also neglected the influence of changes in climate so that we can isolate how tropospheric chemical regimes respond to increased emissions alone. Future increases in temperature and humidity are likely to enhance O_3 loss more than production, reducing the O_3 increases found here [Stevenson *et al.*, 2000], and will also enhance OH production, counteracting future reductions in tropospheric oxidizing capacity and moderating boundary layer OH redistribution. Projected changes in atmospheric circulation and stratospheric O_3 may lead to increased transport of O_3 from the stratosphere [Collins *et al.*, 2003; Shindell *et al.*, 2006], decreasing net O_3 production. More complex interactions, such as the influence of changes in temperature, CO_2 and O_3 on biogenic VOC emissions may also need to be considered. It would be valuable if future studies of

tropospheric composition change diagnose the roles that these processes play in altering the balance of tropospheric photochemistry.

[15] **Acknowledgments.** Both authors contributed equally to this work. P.I.P. acknowledges funding from the Scottish Alliance for Geoscience, Environment and Society (SAGES).

References

- Auvray, M., I. Bey, E. Lull, M. G. Schultz, and S. Rast (2007), A model investigation of tropospheric ozone chemical tendencies in long-range transported pollution plumes, *J. Geophys. Res.*, *112*, D05304, doi:10.1029/2006JD007137.
- Brasseur, G. P., J. T. Kiehl, J.-F. Müller, T. Schneider, C. Granier, X. Tie, and D. Hauglustaine (1998), Past and future changes in global tropospheric ozone: Impact on radiative forcing, *Geophys. Res. Lett.*, *25*, 3807–3810.
- Collins, W. J., R. G. Derwent, B. Garnier, C. E. Johnson, M. G. Sanderson, and D. S. Stevenson (2003), Effect of stratosphere-troposphere exchange on the future tropospheric ozone trend, *J. Geophys. Res.*, *108*(D12), 8528, doi:10.1029/2002JD002617.
- Derwent, R. G., P. G. Simmonds, A. J. Manning, and T. G. Spain (2007), Trends over a 20-year period from 1987 to 2007 in surface ozone at the atmospheric research station, Mace Head, Ireland, *Atmos. Environ.*, *41*, 9091–9098.
- DiNunno, B., D. Davis, G. Chen, J. Crawford, J. Olson, and S. Liu (2003), An assessment of ozone photochemistry in the central/eastern North Pacific as determined from multiyear airborne field studies, *J. Geophys. Res.*, *108*(D2), 8237, doi:10.1029/2001JD001468.
- Eyring, V., et al. (2007), Multi-model simulations of the impact of international shipping on atmospheric chemistry and climate in 2000 and 2030, *Atmos. Chem. Phys.*, *7*, 757–780.
- Gupta, M. L., R. J. Cicerone, and S. Elliott (1998), Perturbation to global tropospheric oxidizing capacity due to latitudinal redistribution of surface sources of NO_x , CH_4 , and CO , *Geophys. Res. Lett.*, *25*, 3931–3934.
- Hudman, R. C., et al. (2004), Ozone production in transpacific Asian pollution plumes and implications for ozone air quality in California, *J. Geophys. Res.*, *109*, D23S10, doi:10.1029/2004JD004974.
- Jaffe, D., H. Price, D. Parrish, A. Goldstein, and J. Harris (2003), Increasing background ozone during spring on the west coast of North America, *Geophys. Res. Lett.*, *30*(12), 1613, doi:10.1029/2003GL017024.
- Lelieveld, J., W. Peters, F. J. Dentener, and M. C. Krol (2002), Stability of tropospheric hydroxyl chemistry, *J. Geophys. Res.*, *107*(D23), 4715, doi:10.1029/2002JD002272.
- Lelieveld, J., J. van Aardenne, H. Fischer, M. de Reus, J. Williams, and P. Winkler (2004), Increasing ozone over the Atlantic Ocean, *Science*, *304*, 1483–1487.
- Marland, G., T. A. Boden, and R. J. Andres (2006), Global, regional, and national fossil fuel CO_2 emissions, <http://cdiac.ornl.gov/trends/emis/overview.html>, Carbon Dioxide Inf. Anal. Cent., Oak Ridge. Natl. Lab., Oak Ridge, Tenn.
- Palmer, P. I., D. J. Jacob, D. B. A. Jones, C. L. Heald, R. M. Yantosca, J. A. Logan, G. W. Sachse, and D. G. Streets (2003), Inverting for emissions of carbon monoxide from Asia using aircraft observations over the western Pacific, *J. Geophys. Res.*, *108*(D21), 8828, doi:10.1029/2003JD003397.
- Parrish, D. D., et al. (2004), Changes in the photochemical environment of the temperate North Pacific troposphere in response to increased Asian emissions, *J. Geophys. Res.*, *109*, D23S18, doi:10.1029/2004JD004978.
- Prather, M., et al. (2001), Atmospheric chemistry and greenhouse gases, in *Climate Change 2001: The Scientific Basis. Contribution of Working*

- Group I to the Third Assessment Report of the Intergovernmental Panel on Climate Change*, edited by J. T. Houghton et al., pp. 239–287, Cambridge Univ. Press, Cambridge, U. K.
- Prather, M., et al. (2003), Fresh air in the 21st century?, *Geophys. Res. Lett.*, *30*(2), 1100, doi:10.1029/2002GL016285.
- Prinn, R. G., et al. (2001), Evidence for substantial variations of atmospheric hydroxyl radicals in the past two decades, *Science*, *229*, 1882–1888.
- Reeves, C. E., et al. (2002), Potential for photochemical ozone formation in the troposphere over the North Atlantic as derived from aircraft observations during ACSOE, *J. Geophys. Res.*, *107*(D23), 4707, doi:10.1029/2002JD002415.
- Shindell, D. T., et al. (2006), Simulations of preindustrial, present-day, and 2100 conditions in the NASA GISS composition and climate model G-PUCCINI, *Atmos. Chem. Phys.*, *6*, 4427–4459.
- Stevenson, D. S., C. E. Johnson, W. J. Collins, R. G. Derwent, and J. M. Edwards (2000), Future estimates of tropospheric ozone radiative forcing and methane turnover: Impact of climate change, *Geophys. Res. Lett.*, *27*, 2073–2076.
- Stevenson, D. S., et al. (2006), Multimodel ensemble simulations of present-day and near-future tropospheric ozone, *J. Geophys. Res.*, *111*, D08301, doi:10.1029/2005JD006338.
- van Aardenne, J. A., F. J. Dentener, J. G. J. Olivier, C. G. M. K. Goldewijk, and J. Lelieveld (2001), A $1^\circ \times 1^\circ$ resolution data set of historical anthropogenic trace gas emissions for the period 1890–1990, *Global Biogeochem. Cycles*, *15*, 909–928.
- Wang, Y. H., and D. J. Jacob (1998), Anthropogenic forcing on tropospheric ozone and OH since preindustrial times, *J. Geophys. Res.*, *103*, 31,123–31,135.
- Wang, J. S., J. A. Logan, M. B. McElroy, B. N. Duncan, I. A. Megretskaja, and R. M. Yantosca (2004), A 3-D model analysis of the slowdown and interannual variability in the methane growth rate from 1988 to 1997, *Global Biogeochem. Cycles*, *18*, GB3011, doi:10.1029/2003GB002180.
- Wild, O., and M. J. Prather (2000), Excitation of the primary tropospheric chemical mode in a global 3-D model, *J. Geophys. Res.*, *105*, 24,647–24,660.
- Wild, O., et al. (2004), Chemical transport model ozone simulations for spring 2001 over the western Pacific: Regional ozone production and its global impacts, *J. Geophys. Res.*, *109*, D15S02, doi:10.1029/2003JD004041.

P. I. Palmer, School of GeoSciences, University of Edinburgh, King's Buildings, West Mains Road, Edinburgh, EH9 3JN, UK. (pip@ed.ac.uk)
O. Wild, Department of Environmental Science, Lancaster Environment Centre, Lancaster University, Lancaster, LA1 4YQ, UK. (o.wild@lancaster.ac.uk)